ELSEVIER

0010-4485(95)00068-2

Computer-Aided Design, Vol. 28, No. 6/7, pp. 539–549, 1996

0010-4485/96 $15.00 + 0.00

Determining intersection curves between surfaces of two solids

K Abdel-Malek and H J Yeh

Intersection curves between two parametric surfaces are numerically computed using continuation methods. A starting point to initiate the algorithm is determined using the Moore–Penrose pseudo-inverse. Singularities along the curve are detected using a row-rank deficiency of the Jacobian. At singular points where two or more curves intersect, bifurcation points are calculated. To numerically compute a multiple of curves at a bifurcation point, a 2nd-order expansion method is used to render the equation into a quadratic form, such that the tangents are computed. The solution is then switched to a bifurcation branch. The method is demonstrated for two intersecting surfaces having two intersecting curves. The method is also validated for special cases through a number of examples. Copyright © 1996 Elsevier Science Ltd

Keywords: intersections, geometric modelling, interference, continuation methods

INTRODUCTION

This paper presents a method for determining the intersection curves of two intersecting parametric surfaces. In the field of computer-aided geometric design, these curves are called trimming curves. The problem of numerically determining the trimming curve is complicated when several curves exist. In addition, most numerical algorithms require the estimation of a starting point on or close to the solution curve. Muellenheim[1] has presented an iterative method for calculating a starting point that is close to a solution curve. The starting point has also been computed using lattice and subdivision methods[2]. General intersection problems have been addressed by Barnhill *et al.*[2], Barnhill and Kersey[3], Seredeberg[5] and Farouki[4]. Lattice evaluation methods were used to determine the intersection curve[6,7]. Reviews of general intersection methods are numerous[8–11]. Wilf and Manor[12] presented a method using a modification of Levin's ruled-surface parametrization scheme, guided by invariant-factors classification and furthermore, by factorization of the parametrization polynomials.

A procedural method for evaluating the intersection curve was also presented[13]. The same problem was formulated and solved using parallel computing algorithms[14]. Using parallelism, the authors report a significant speed-up in computing. Another parallel algorithm using the divide-and-conquer method was presented by Burger and Schaback[15]. The computational complexity of this algorithm was also analysed. Search techniques were used to refine the interval progressively[16]. Other methods that were applied to the surface–surface intersection problem include a topological and differential-equation method[17]. In this method, the vector field defined as the gradient of the oriented distance function is used to detect critical points in the field such as singularities. Tensorial differential equations are then used to trace intersection segments. Another method that uses unidimensional searches to detect intersection points was presented by Aomura and Uehara[18].

A different approach of higher-dimensional formulation including offsets, equal distance surfaces, and variable radius blending surfaces was discussed by Hoffman[19] and Hoffman[20]. Higher-dimensional formulation was also used by Chuang[21] to determine a local and global approximant.

Marching methods have been extensively used by researchers in this field[4,9,22]. The accuracy of marching methods has been improved by proper control of the step size[23]. Marching through singularities using birational transformations have been presented by Bajaj *et al.*[22] Singularities were also analysed by Owen and Rockwood[24] by locally constructing a 2nd-order approximant to each surface.

In this paper, the curve is traced using the so-called continuation methods[25–29]. This problem is formulated into one constraint equation that allows the use of the Moore–Penrose pseudo-inverse to determine a starting point on the curve. This method relies upon a row-rank deficiency of the Jacobian to determine bifurcation points. In many cases, however, a multiple of intersection curves pass through one point. Thus, the problems of finding this point and switching solutions to another branch are addressed.

Department of Mechanical Engineering and Center for Computer Aided Design, The University of Iowa, Iowa City, IA 52242, USA
Paper received: 11 April 1995. Revised: 18 July 1995

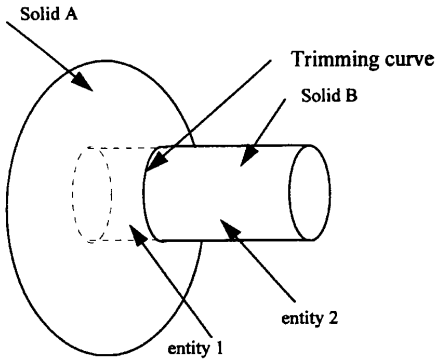

Figure 1 The trimming curve (intersection curve) between two parametric surfaces

SURFACE INTERSECTION

Boundary representation (B-rep) methods are used by many CAD systems to model engineering structures and machines[11,30]. Complicated solids are modelled by providing the surfaces and their geometric boundaries satisfying certain geometric and topological requirements[11]. In order to complete the description of a solid, trimming curves in terms of the intersecting surfaces are computed.

The B-rep method uses a topological description of the connectivity and orientation of vertices, edges and faces, and a geometric description for embedding these surface elements in space. A survey of various representation methods can be found in Hoffman's book[11].

Consider a solid that is to be represented by a number of parametric surfaces ${}^{A}\mathbf{x}_i(u,v):U\subset R^2\rightarrow R^3$, ${}^{A}\mathbf{x}_i=\{{}^{A}\mathbf{x}_1\ {}^{A}\mathbf{x}_2\ \ldots\}$ which is a differentiable map ${}^{A}\mathbf{x}_i$ from an open set $U\subset R^2$ into R^3. That is, the vectors $\partial {}^{A}\mathbf{x}_i/\partial u$ and $\partial {}^{A}\mathbf{x}_i/\partial v$ are linearly independent. The independence of these vectors is necessary to guarantee a nonvanishing Jacobian.

To determine trimming curves created by the intersection of two surfaces, it is necessary to compute the intersection curve between any two surfaces. *Figure 1* illustrates a solid represented by two intersecting surfaces. The intersection curve (trimming curve) is also shown in *Figure 1*.

The problem of calculating the intersection curve between two surfaces is one of the most important computational tasks in several engineering applications such as in geometric modelling, CAD/CAM, computer animation and robotics. Many methods for computing the intersection curves between general surfaces have been derived in the past. Pratt and Geisow[8] and Barnhill[10] summarize and briefly distinguish most of those techniques into five main categories, namely algebraic, lattice evaluation, marching, recursive subdivision, and continuation methods. In this section, only surfaces represented parametrically are treated. A surface is parameterized as

$$\mathbf{x}^1(u,v) \tag{1}$$

with constrained parameters as

$$u_1\le u\le u_2 \tag{2}$$

$$v_1\le v\le v_2 \tag{3}$$

The second surface is parametrized as

$$\mathbf{x}^2(s,t) \tag{4}$$

with constrained parameters as

$$s_1\le s\le s_2 \tag{5}$$

$$t_1\le t\le t_2 \tag{6}$$

where (u,v) and (s,t) are the independent parametric coordinates. To impose the inequality constraints in numerical form, it is convenient to parametrize the above constraints by introducing new generalized coordinates λ_i such that an inequality constraint of the form

$$q_i^{\min}\le q_i\le q_i^{\max} \tag{7}$$

can be parametrized by introducing a new generalized coordinate λ_i as

$$q_i=a_i+b_i\sin\lambda_i \tag{8}$$

where $a_i=(q_i^{\max}+q_i^{\min})/2$ and $b_i=(q_i^{\max}-q_i^{\min}/2$ are the mid-point and half-range of the inequality constraint.

In this paper, the computation scheme of the disjoint branches of the intersection curve is divided into two phases: (1) finding the starting point, and (2) tracing along the intersection curve. The case where a singularity (so-called bifurcation) occurs is also discussed. Switching solutions by calculating tangents at a bifurcation point is also addressed.

FINDING A STARTING POINT

For the case of interference of surfaces that results in disjoint branches, it is a nontrivial task to find an initial point on the intersection curve. The method presented in this paper involves starting from an initial guess $\mathbf{q}^1$, on one of the surfaces, to determine a starting point $\mathbf{q}^*$ on an intersection curve. The intersection problem may be considered as solving the system of seven nonlinear equations with eight variables where the constraint function $\mathbf{H}(\mathbf{q})$ is

$$\mathbf{H}(\mathbf{q})=\begin{bmatrix}\mathbf{x}^1(u,v)-\mathbf{x}^2(s,t)\\ u-[(u_1+u_2)/2+\sin(\lambda_1)(u_2-u_1)/2]\\ v-[(v_1+v_2)/2+\sin(\lambda_2)(v_2-v_1)/2]\\ s-[(s_1+s_2)/2+\sin(\lambda_3)(s_2-s_1)/2]\\ t-[(t_1+t_2)/2+\sin(\lambda_4)(t_2-t_1)/2]\end{bmatrix}=\mathbf{0} \tag{9}$$

where $\mathbf{q}=\{u\ v\ s\ t\ \lambda_1\ \lambda_2\ \lambda_3\ \lambda_4\}$ and the inequality constraints of Equations 2, 3, 5, and 6 were parametrized per Equation 8. The Jacobian of the constraint function $\mathbf{H}(\mathbf{q})$ for a certain configuration $\mathbf{q}^1$ is the 3×3 matrix

$$\mathbf{H}_{\mathbf{q}}(\mathbf{q}^1)=\left[\frac{\partial H_i}{\partial q_j}(\mathbf{q}^1)\right] \tag{10}$$

To satisfy the constraint equation, an algorithm similar to the Newton–Raphson iteration method is employed, as follows:

$$\mathbf{H}_q \Delta \mathbf{q} = -\mathbf{H} \tag{11}$$

If the constraint subJacobian matrix is square then Equations 9 and 11 comprise the conventional Newton–Raphson iteration method, with its well-known quadratic convergence properties[26].

The constraint equation (Equation 9) has more rows than columns and the constraint subJacobian $\mathbf{H}_q$ has more columns than rows, thus Equation 11 has multiple solutions. One solution to this type of problem is to find the solution $\Delta \mathbf{q}$ with minimum norm[28,31]; i.e. to solve the minimization problem

$$\min \frac{1}{2} \Delta \mathbf{q}^T \Delta \mathbf{q} \tag{12}$$

$$\mathbf{H}_q \Delta \mathbf{q} = -\mathbf{H} \tag{13}$$

Using the Lagrange multiplier approach that appends a multiplier vector times the equations to be satisfied to the function that is to be minimized, define

$$\Psi \equiv \frac{1}{2} \Delta \mathbf{q}^T \nabla \mathbf{q} - \lambda^T (\mathbf{H}_q \Delta \mathbf{z} + \mathbf{H}) \tag{14}$$

As a necessary conditon for a solution of the minimization problem (Equation 11), the gradient of the function in Equation 14 is set to zero, yielding

$$\Delta \mathbf{q}^T = \boldsymbol{\lambda}^T \mathbf{H}_q \tag{15}$$

or,

$$\Delta \mathbf{q} = \mathbf{H}_q^T \boldsymbol{\lambda} \tag{16}$$

Substituting this result into the linearized constraint equation of Equation 11 yields

$$\mathbf{H}_q \mathbf{H}_q^T \boldsymbol{\lambda} = -\mathbf{H} \tag{17}$$

If the subJacobian $\mathbf{H}_q$ has full row rank, then the coefficient matrix on the left of Equation 17 is nonsingular. In fact, it is positive definite. Therefore,

$$\boldsymbol{\lambda} = \left(\mathbf{H}_q \mathbf{H}_q^T\right)^{-1} (-\mathbf{H}) \tag{18}$$

Substituting this result into Equation 16 yields the result

$$\Delta \mathbf{q} = \mathbf{H}_q^T \left(\mathbf{H}_q \mathbf{H}_q^T\right)^{-1} (-\mathbf{H}) \tag{19}$$

where the coefficient matrix on the right is the so-called Moore–Penrose pseudo-inverse of the subJacobian[13]. Starting with an initial guess $\mathbf{q}^1$, the update of generalized coordinates is calculated through

$$\Delta \mathbf{q} = \mathbf{H}_q^* (-\mathbf{H}) \tag{20}$$

where $\mathbf{H}_q^*$ is the Moore–Penrose pseudo-inverse of the Jacobian $\mathbf{H}_q$, defined by Equation 19 as

$$\mathbf{H}_q^* = \mathbf{H}_q^T \left(\mathbf{H}_q \mathbf{H}_q^T\right)^{-1} \tag{21}$$

Rather than computing the inverse implied in Equation 21, define

$$\mathbf{y} \equiv \left(\mathbf{H}_q \mathbf{H}_q^T\right)^{-1} (-\mathbf{H}) \tag{22}$$

which is equivalent to solving the matrix equation

$$\left(\mathbf{H}_q \mathbf{H}_q^T\right) \mathbf{y} = -\mathbf{H} \tag{23}$$

Numerically solving this equation for $\mathbf{y}$ and substituting the result into Equaiton 19 yields

$$\Delta \mathbf{q} = \mathbf{H}_q^T \mathbf{y} \tag{24}$$

Carrying out the Moore–Penrose pseudo-inverse iteration using Equations 23 and 24, yields a process that has the same quadratic convergence characteristics as the standard Newton–Raphson method[32].

Using this procedure, the starting point $\mathbf{q}^*$ on the intersection curve can be found within a few iterations without adding any new constraint equations. Although this method can quickly converge the initial guess into a starting point, only one starting point will be found, and only the corresponding intersection curve can be traced. If disjoint branches of the curve exist, other starting points should be obtained. In this case, further study of branching from the bifurcation point is necessary.

TRACING ALONG THE CURVE

Once the starting point is found, subsequent points on the intersection curve can be traced along the tangent direction by using the so-called continuation method[27]. The idea is to introduce a new constraint equation. Suppose the parametric coordinates of the starting point $\mathbf{q}^*$ are (u_0, v_0) and (s_0, t_0). The tangent vector $\mathbf{t}(\mathbf{H}_q(\mathbf{q}))$ to the set defined by $\mathbf{H}(\mathbf{q}) = \mathbf{0}$ is uniquely defined by

$$\mathbf{H}_q \mathbf{t}(\mathbf{H}_q) = \mathbf{0} \tag{25}$$

the normalization

$$\|\mathbf{t}(\mathbf{H}_q)\|_2 = 1 \tag{26}$$

and

$$\det \begin{bmatrix} \mathbf{H}_q \\ \mathbf{t}(\mathbf{H}_q)^T \end{bmatrix} > 0 \tag{27}$$

where Equations 25–27 were set forth to define a unique tangent in the Predictor–Corrector method[32]. The geometric interpretation of the step marching procedure is shown in *Figure 2a*. A well-established numerical code (called PITCON[25]) that implements this continuation method is used to perform the tracing.

By setting the new point as the current point, the unique tangent vector is computed at each point along the curve. The tracing is continued until one of two cases occurs: (1) the boundary is reached, or (2) return-

ing to the starting point. Note however, that if more than one intersection curve exists, only one is traced.

SINGULARITY / BIFURCATION

Often more than one intersection curve exists. If the curves are disjoint branches and do not intersect (e.g. two parallel cylinders intersecting), a grid search method[33] is used in the $u\nu$-space to locate the other branch. If the two branches intersect at a point, this point is called a bifurcation point. This may occur for a number of reasons, the most general of which is common tangents. In order to have a complete representation of all intersection curves, it is necessary to detect a bifurcation point along a solution curve (other methods can be found in Keller[26] and Rheinboldt[25]). In addition, it is required to numerically switch from the curve onto the second solution branch. This section will consider singular bifurcation points. Treatment of higher-order bifurcation points can be found in Golubitsky *et al.*[34]

Allgower and Georg[27] proved that if the bifurcation point $\mathbf{q}^o$ is a simple bifurcation point of the equation $\mathbf{H}(\mathbf{q}^o) = \mathbf{0}$, then the determinant of the following augmented Jacobian changes sign at the singularity.

$$\text{sign det}\begin{bmatrix} \mathbf{H}_q \\ \mathbf{t}(\mathbf{H}_q)^T \end{bmatrix} \tag{28}$$

where $\mathbf{t}(\mathbf{H}_q)$ is the tangent function to the set defined by $\mathbf{H}(\mathbf{q}) = \mathbf{0}$ for $\mathbf{H}:\mathbf{R}^n \rightarrow \mathbf{R}^{n-1}$. In practice, Equation 28 can be executed by monitoring the Jacobian $\mathbf{H}_q$ for where it becomes row rank deficient of degree one at a bifurcation point $\mathbf{q}^o$ such that

$$\text{Rank}\left(\mathbf{H}_q(\mathbf{q}^o)\right) = n - 2 \tag{29}$$

At such a point, a pair of solution curves pass through the point. Having determined that there is a single bifurcation point, it is of interest to determine this special point. This can be done by changing the step size of the continuation algorithm while monitoring the sign of Equation 28. Elementary row matrix operations may be performed to reduce the Jacobian matrix $\mathbf{H}_q$ to the form

$$\mathbf{E}\left(\mathbf{H}_q(\mathbf{q}^o)\right) = \begin{bmatrix} \mathbf{F}_q(\mathbf{q}^o) \\ \mathbf{0} \end{bmatrix} \tag{30}$$

where $\mathbf{F}_q(\mathbf{q}^o)$ is an $(n-2)\times n$ matrix with full row rank. Since the transformation $\mathbf{E}$ involves only interchanging equation order, multiplying an equation by a nonzero constant and adding one equation to another, if does not change the solution set. Thus Equation 9 may be transformed to

$$\tilde{\mathbf{H}}(\mathbf{q}) \equiv \begin{bmatrix} \mathbf{F}(\mathbf{q}) \\ f(\mathbf{q}) \end{bmatrix} \equiv \mathbf{E}(\mathbf{H}(\mathbf{q})) = \mathbf{0} \tag{31}$$

which yields the modified continuation equation as $\tilde{\mathbf{H}}(\mathbf{q}) = \mathbf{0}$. Since only elementary row operations have been used, the lower submatrix on the right is indeed its Jacobian. Since the rank of $\mathbf{F}_q(\mathbf{q}^o)$ is of dimension $(n-2)$, the null space of $\mathbf{F}_q(\mathbf{q}^o)$ is of dimension two, yielding two nonzero solutions of

$$\mathbf{F}_q(\mathbf{q}^o)\boldsymbol{\tau}_i = \mathbf{0} \quad i = 1,2 \tag{32}$$

where the two vectors $\boldsymbol{\tau}_i$ may be orthonormalized such as

$$\boldsymbol{\tau}_i^T\boldsymbol{\tau}_i = \delta_{ij} \quad i,j = 1,2 \tag{33}$$

Thus, the objective is to find tangent vectors $\mathbf{t}(\mathbf{H}_q)$ continuation curves at $\mathbf{q}^o$ of the form

$$\mathbf{t}(\mathbf{H}_q) = \sum_{j=1}^{3} \alpha_j\boldsymbol{\tau}_j = \alpha_j\boldsymbol{\tau}_j \tag{34}$$

To be tangent to the solution curve, the equation governing the solution curve should be satisfied to lowest, nontrivial order Taylor approximation, i.e.

$$\tilde{\mathbf{H}}\left(\mathbf{q}^o + \mathbf{t}(\mathbf{H}_q)\right) \sim \tilde{\mathbf{H}}(\mathbf{q}^o) + \begin{bmatrix} \mathbf{F}(\mathbf{q}^o)\alpha_j\boldsymbol{\tau}_j \\ \frac{1}{2}(\alpha_l\boldsymbol{\tau}_l^T)f_{qq}(\mathbf{q}^o)\alpha_k\boldsymbol{\tau}_k \end{bmatrix} = (\tag{35}$$

where the Hessian of $f(\mathbf{q})$, evaluated at $\mathbf{q}^o$ is

$$f_{qq}(\mathbf{q}^o) \equiv \left[\frac{\partial^2 f(\mathbf{q}^o)}{\partial q_i \partial q_j}\right] \tag{36}$$

The 2nd-order Taylor approximation is required, since its 1st-order Taylor terms are identically zero. Since the

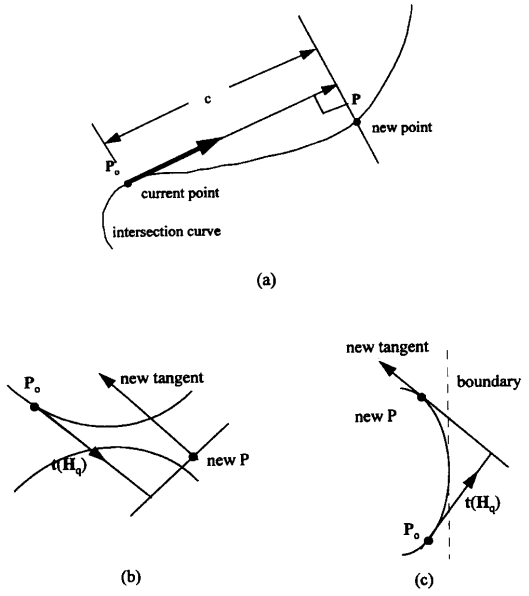

Figure 2 (a) The step marching procedure for tracing the curve, (b) tangents in opposite directions, (c) tangent is not in opposite directions

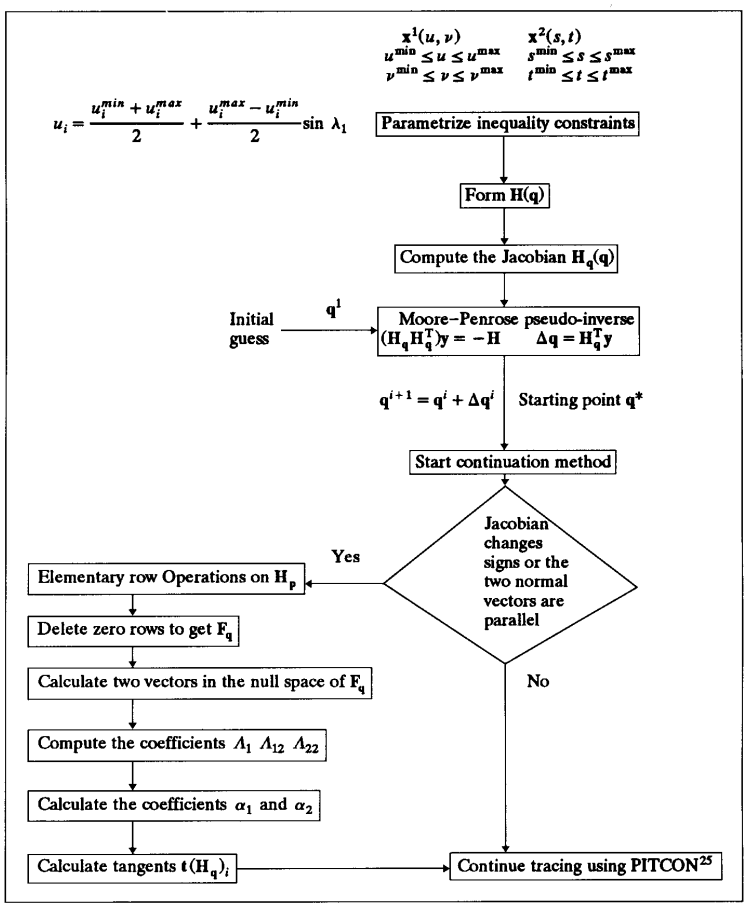

upper subvector on the right of Equation 31 is zero, for all α_j, Equation 31 reduces to

$$\boldsymbol{\alpha}^T \boldsymbol{\Lambda}\, \alpha = \mathbf{0} \tag{37}$$

where $\boldsymbol{\alpha} = [\alpha_1 \ \alpha_2]^T$ and

$$\boldsymbol{\Lambda} = \left[\boldsymbol{\tau}_i^T f_{qq}(\mathbf{q}^o)\boldsymbol{\tau}_j\right] = [\Lambda_{ij}] \tag{38}$$

The quadratic equation (Equation 37) may be transformed to a quadratic equation in the ratio of the two variables such that

$$\Lambda_{11}\left(\frac{\alpha_1}{\alpha_2}\right)^2 + 2\Lambda_{12}\left(\frac{\alpha_1}{\alpha_2}\right) + \Lambda_{22} = 0 \tag{39}$$

To determine a pair of values for α_1 and α_2 that define distinct tangents, the solution is sought such that

$$\frac{\alpha_1}{\alpha_2} = -\frac{\Lambda_{12}}{\Lambda_{11}} \pm \frac{1}{\Lambda_{11}}\sqrt{\Lambda_{12}^2 - \Lambda_{11}\Lambda_{22}} \quad \text{for } \Lambda_{11} \neq 0 \text{ and } \Lambda_{22} \neq 0 \tag{40}$$

If $\Lambda_{11} = 0$ and $\Lambda_{22} = 0$ and $\Lambda_{12} \neq 0$ the solutions are $\boldsymbol{\alpha}^1 = [1\ 0]^T$ and $\boldsymbol{\alpha}^2 = [0\ 1]^T$. In the analysis by Lukacs[35], the curvature of the intersection curve is studied. In order to determine whether a point along the traced curve exhibits singular behaviour, the eigenvalues λ_1 and λ_2, associated with the quadratic equation are studied. The following four cases may arise.

(1) If λ_1 and λ_2 have the same sign, then the point is isolated.
(2) If λ_1 and λ_2 have opposite signs, then there are two tangents at this singular point.
(3) If λ_1 or λ_2 equals zero, then there is one branch passing through this point.
(4) If λ_1 and λ_2 are zero, then this point is 2nd-order singularity.

Similarly, three cases arise from studying the quadratic function of Equation 39.

(1) If α_1 and α_2 are two real numbers, then there are two distinct tangents at a singular point.
(2) If α_1 or α_2 equals zero, then only one curve passes through this point.
(3) If α_1 or α_2 is imaginary, no real tangents can be computed.

In the preceding tracing process, when the trace crosses over the singular point, the determinant of the Jacobian matrix changes signs. In this case, the new tangent of the computed point is inspected to determine whether it orients in opposite direction (within a tolerance) with the previous tangent. If this occurs, the new step size c must change signs, as shown in *Figure 2b*, such that the tracing continues without retracing. *Figure 2c* depicts another situation where the determinant changes signs but the computed tangent will not point in the opposite direction.

ALGORITHM

The following algorithm is presented to illustrate the discussion

The following example will be discussed in detail to illustrate the algorithm. Consider the intersection of two cylinders of two different sizes. The surfaces of the larger cylinder is parametrized as

$$\mathbf{x}^1(u,v) = \begin{bmatrix} 10\cos u + 5 \\ v \\ -10\sin u \end{bmatrix} \tag{41}$$

and has inequality constraints as

$$0 \le u \le 2\pi \tag{42}$$

$$-20\sqrt{3} \le v \le 20\sqrt{3} \tag{43}$$

The smaller cylinder is parametrized as

$$\mathbf{x}^2(s,t) = \begin{bmatrix} 5\cos s \\ 2.5\sin s + (\sqrt{3}/2)t \\ -2.5\sqrt{3}\sin s + (t/2) \end{bmatrix} \tag{44}$$

and has inequality constraints as

$$0 \le s \le 2\pi \tag{45}$$

$$-40 \le t \le 40 \tag{46}$$

The two cylinders are shown in *Figure 3a*. The constraint function is

$$\mathbf{H}(\mathbf{q}) = \begin{bmatrix} 10\cos u + 5 - 5\cos s \\ v - 2.5\sin s - \dfrac{\sqrt{3}}{2}t \\ -10\sin u + 2.5\sqrt{3}\sin s - 0.5t \\ u - \pi - \pi\sin\lambda_1 \\ v - 0 - 20\sqrt{3}\sin\lambda_2 \\ s - \pi - \pi\sin\lambda_3 \\ t - 0 - 40\sin\lambda_4 \end{bmatrix} = \mathbf{0} \tag{47}$$

This is a one degree of freedom system with seven equations and eight unknows. The Jacobian of $\mathbf{H}$ is 7×8 matrix. To determine the trimming curve, a starting point is needed. The Moore–Penrose pseudo-inverse is used. This algorithm requires an initial guess of a point on one of the surfaces. An initial guess for a

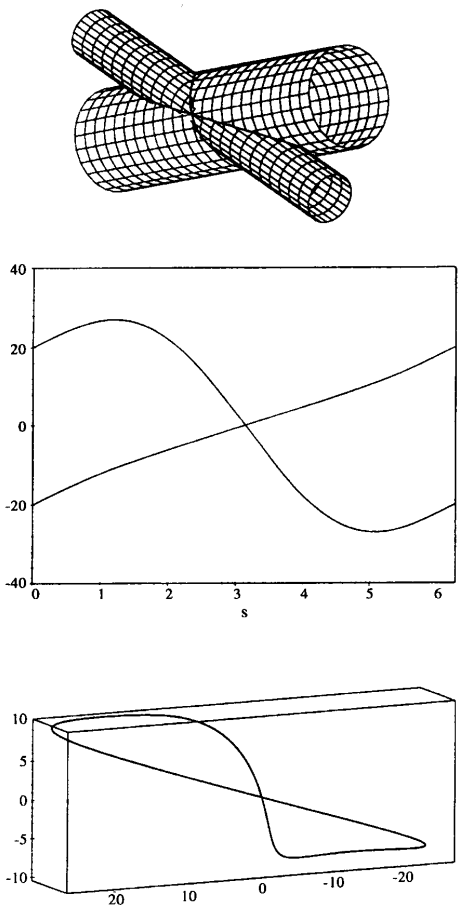

Figure 3 (a) Two intersecting cylinders, (b) computed intersection curves

point (on one of the surfaces) is given as

$$\mathbf{q}^1 = [\pi/2 \quad -20 \quad \pi/2 \quad -17.32 \quad -\pi/6 \quad -\pi/6 \quad -\pi/6 \quad -\pi/6]^T$$

Using the Moore–Penrose method a starting point (on the curve of intersection) is computed after five iterations as

$$\mathbf{q}^* = [1.870 \quad -7.412 \quad 1.151 \quad -11.19 \quad -0.416 \quad -0.186 \quad -0.686 \quad -0.329]^T$$

Tracing continues until the Jacobian changes signs at

$$\mathbf{q}^\circ = [3.142 \; 0.301 \times 10^{-8} \; 3.142 \; 0.736 \times 10^{-8} \; 0.302 \times 10^{-9} \; 0.755 \times 10^{-10} \; 0.427 \times 10^{-9} \; 0.214 \times 10^{-9}]^T$$

At $\mathbf{q}^\circ$, the Jacobian $\mathbf{H}_q(\mathbf{q}^\circ)$ is row-rank deficient, thus, $\mathbf{q}^\circ$ is a singular point. Performing elementary row operations, the Jacobian is reduced to

$$\mathbf{E}(\mathbf{H}_q(\mathbf{q}^\circ)) = \begin{bmatrix} \mathbf{F}_q(\mathbf{q}^\circ) \\ \mathbf{0} \end{bmatrix} \tag{48}$$

The first row of $\mathbf{H}_q(\mathbf{q}^o)$ has all zero elements. The first row is deleted to form $\mathbf{F}_q$, which has full rank

$$\mathbf{F}_q = \begin{bmatrix} 0 & 1 & 2.5 & -0.866 & 0 & 0 & 0 & 0 \\ 10 & 0 & -4.33 & -0.5 & 0 & 0 & 0 & 0 \\ 1 & 0 & 0 & 0 & -3.142 & 0 & 0 & 0 \\ 0 & 1 & 0 & 0 & 0 & -40 & 0 & 0 \\ 0 & 0 & 1 & 0 & 0 & 0 & -3.142 & 0 \\ 0 & 0 & 0 & 1 & 0 & 0 & 0 & -34.641 \end{bmatrix} \tag{49}$$

where $\mathbf{F}_q$ has rank $(n-2)$.

Two distinct nonzero solutions of $\mathbf{F}_q\boldsymbol{\tau}^i = 0$ $(i = 1, 2)$ can be computed such that

$$\boldsymbol{\tau}_1 = [-0.173\ 1.000\ -0.400\ 0\ -0.055\ 0.025\ -0.127\ 0]^T$$

and

$$\boldsymbol{\tau}_2 = [-0.200\ 0.0\ -0.346\ 1.000\ 0.0637\ 0\ 0.110\ 0.029]^T$$

Since the first row of $\mathbf{H}_q$ is zero and was deleted, the first constraint term of of $\mathbf{H}_q$ is

$$f(\mathbf{q}) = 10\cos u + 5 - 5\cos s \tag{50}$$

The $n \times n$ Hessian matrix f_{qq} is determined and the coefficients Λ_{11}, Λ_{22} are computed as

$$\Lambda_{11} = \boldsymbol{\tau}_1^T f_{qq}(\mathbf{q}^o)\boldsymbol{\tau}_1 = -0.5 \tag{51}$$

$$\Lambda_{12} = \boldsymbol{\tau}_1^T f_{qq}(\mathbf{q}^o)\boldsymbol{\tau}_2 = 0.346 \tag{52}$$

$$\Lambda_{22} = \boldsymbol{\tau}_2^T f_{qq}(\mathbf{q}^o)\boldsymbol{\tau}_2 = -0.2 \tag{53}$$

Substitute these coefficients into the quadratic equation

$$\Lambda_{11}\left(\frac{\alpha_1}{\alpha_2}\right)^2 + 2\Lambda_{12}\left(\frac{\alpha_1}{\alpha_2}\right)^2 + \Lambda_{22} = 0 \tag{54}$$

two solutions are computed

$$\alpha_1 = 0.410\alpha_2 \tag{55}$$

and

$$\alpha_1 = 0.975\alpha_2 \tag{56}$$

Setting $\alpha_2 = 1.0$, two solutions for the α-coefficients are obtained

$$\alpha_1 = 0.410,\ \alpha_2 = 1.0$$

and

$$\alpha_1 = 0.976,\ \alpha_2 = 1.0$$

Two distinct tangent vectors $\mathbf{t}(\mathbf{H}_q) = \alpha_1\boldsymbol{\tau}_1 + \alpha_2\boldsymbol{\tau}_2$ at this bifurcation point are calculated. The two normalized tangents are

$$\mathbf{t}(\mathbf{H}_q)_1 = [0.116\ 0.371\ 0.165\ 0.904\ 0.0371\ 0.009\ 0.053\ 0.026]^T$$

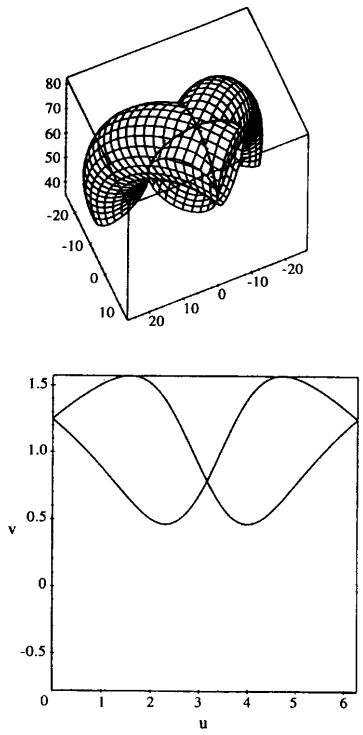

Figure 4 (a) Two intersecting surfaces (torus), (b) intersection curves in the uv space

and

$$\mathbf{t}(\mathbf{H}_q)_2 = [0.022\ 0.697\ -0.031\ 0.715\ 0.007\ 0.017\ -0.099\ 0.021]^T$$

Since both tangents have been computed, the tracing can be continued. The intersection curve is shown in *Figure 3b*, and the 3D curve is shown in *Figure 3c*.

NUMERICAL EXAMPLES

Example 1

To illustrate the determination of surfaces enveloping a solid using the method outlined above, consider the two surfaces depicted in *Figure 4a*. The equation of the first surface is given as

$$\mathbf{x}^1(u, v) = \begin{bmatrix} 7.07\cos u\cos v + 7.07(\sin u - \sin v) \\ +14.14\cos v \\ -7.07\cos u\cos v \\ +7.07(\sin u + \sin v) - 14.14\cos v \\ \quad 10\cos u\sin v + 10\cos v \\ +20\sin v + 50 \end{bmatrix} \tag{57}$$

with inequality constraints defined as

$$0 \le u \le 2\pi \tag{58}$$

$$-0.785 \le v \le 1.57 \tag{59}$$

and the parametrization of the second surface is given as

$$\mathbf{x}^1(u,v) = \begin{bmatrix} -7.07\cos s\cos t + 7.07(\sin s + \sin t) \\ \quad -14.14\cos t \\ -7.07\cos s\cos t - 7.07(\sin s - \sin t) \\ \quad -14.14\cos t \\ 10\cos s\sin t + 10\cos t + 20\sin t + 50 \end{bmatrix} \tag{60}$$

with inequality constraints as

$$0 \le s \le 2\pi \tag{61}$$

$$-0.785 \le t \le 1.57 \tag{62}$$

The starting $\mathbf{q}^*$ computed using the Moore–Penrose pseudo-inverse is

$$\mathbf{q}^* = [0.6184\ 3.4086\ 0.6184\ 2.8745\ 0.1928\ 0.0851\ 0.1928\ -0.0851]$$

Using this point as a starting point for mapping continuation curves, a singular bifurcation point is encountered at

$$\mathbf{q}^0 = [0.7854\quad 3.1416\quad 0.7854\quad 3.1416\quad 0.3398\quad 0.8306\times 10^{-9}\quad 0.3398\quad -0.8306\times 10^{-9}]$$

The tangents computed in the uv space at the bifurcation point are $\mathbf{t}(\mathbf{H}_q)_1 = [0.5773\ 0.8165]^T$ and $\mathbf{t}(\mathbf{H}_q)_2 = [-0.5774\ 0.8165]^T$. The resulting intersecting curves in the uv space are depicted in *Figure 4b*.

Example 2

Figure 5a depicts the surface of a torus parametrized as

$$\mathbf{x}^1(u,v) = \begin{bmatrix} (10 - 5\sin u)\sin v \\ 5\cos u \\ (10 - 5\sin u)\cos v \end{bmatrix} \tag{63}$$

subject to the following inequality contraints

$$0 \le u \le 2\pi \tag{64}$$

$$0 \le v \le 2\pi \tag{65}$$

and the surface of a cylinder parametrized as

$$\mathbf{x}^2(s,t) = \begin{bmatrix} t \\ 5\cos s \\ 5\sin s \end{bmatrix} \tag{66}$$

subject to the following inequality constraints

$$0 \le s \le 2\pi$$

$$-20 \le t \le 20$$

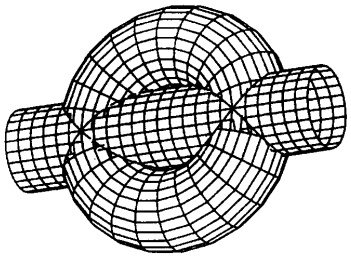

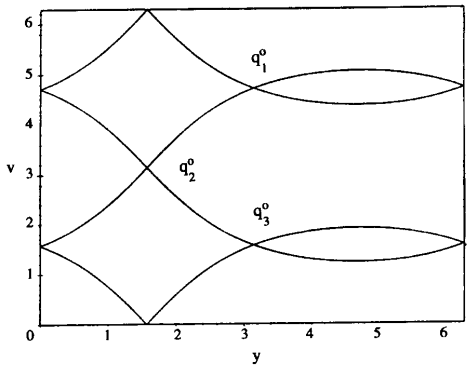

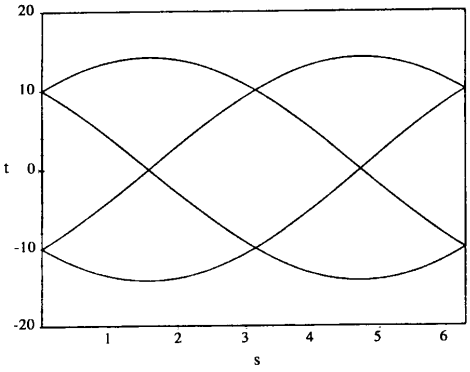

Figure 5 (a) The intersection of a torus and a cylinder, (b) intersection curves in the uv space depicting bifurcation points, (c) intersection curves in the st space

In order to compute a staring point on the curve of intersection, an initial guess of a point on the surface is specified. Using the Moore–Penrose pseudo-inverse, the computed starting point is

$$\mathbf{q}^* = [2.423\ 5.225\ 2.423\ -5.843\ 18.618\ 57.273\ 18.618\ -44.279]^T$$

During the continuation technique used, three singular points are computed:

(1) The first singular point is $\mathbf{q}_1^o = [u\ v\ s\ t] = [3.141\ 4.712\ 3.141\ -9.999]^T$ Two tangents are computed at this point such that $\mathbf{t}(\mathbf{H}_q)_1 = [-4.472\ -2.236]^T$ and $\mathbf{t}(\mathbf{H}_q)_2 = [-4.472\ 2.236]^T$.

(2) The second singular point is $\mathbf{q}_2^\circ = [1.571\ 3.141\ 4.712\ -0.787 \times 10^{-8}]^T$ and two tangent vectors are calculated $\mathbf{t}(\mathbf{H}_q)_1 = [2.236\ 3.162]^T$ and $\mathbf{t}(\mathbf{H}_q)_2 = [2.236\ -3.162]^T$.

(3) The third singular point is $\mathbf{q}_3^\circ = [3.141\ 1.571\ 9.999]^T$ and the two tangent vectors are calculated accordingly as $\mathbf{t}(\mathbf{H}_q)_1 = [-4.472\ -2.236]^T$ and $\mathbf{t}(\mathbf{H}_q)_2 = [-4.472\ 2.236]^T$. The resulting intersection curves depicting the three bifurcation points are shown in the uv space in *Figure 5b*. The curve in the st space is shown in *Figure 5c*.

EVALUATION OF SPECIAL CASES

An evaluation of the algorithm's performance on two special cases similar to those discussed by Barnhill[10] are presented. The two cases are: (1) the contact of a surface with another at a very small region and (2) the intersection along a generatrix of two surfaces.

The intersections, in the method discussed in Barnhill[10], are established by fitting curves through exact points which are the intersections between one surface and the isoparametric curves from the other surface. An iterative approach is presented for searching.

The region of intersection is very small

This example is one that was discussed in Barnhill[10]. The intersection loop is very small compared to the dimensions of both surfaces. A sphere touching the surface of a plane is considered as shown in *Figure 6*. The surface of the sphere is parametrized as

$$\mathbf{x}^1(\theta, \varphi) = \begin{bmatrix} \cos\theta\cos\varphi \\ \sin\theta\sin\varphi \\ \sin\varphi \end{bmatrix}, 0 \le \theta \le 2\pi, -\frac{\pi}{2} \le \varphi \le \frac{\pi}{2} \tag{67}$$

and the surface of the sphere is parametrized as

$$\mathbf{x}^2(s,t) = \begin{bmatrix} s \\ 1.0 \\ t \end{bmatrix}, -1 \le s \le 1, -1 \le t \le 1 \tag{68}$$

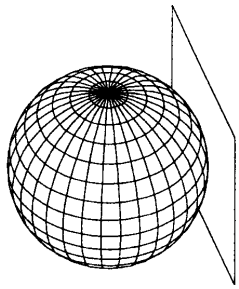

Figure 6 Intersection of a surface with another at a very small region

The constraint function is

$$\mathbf{H}(\mathbf{q}) = \begin{bmatrix} \cos\theta\cos\varphi - s \\ \sin\theta\cos\varphi - 1 \\ \sin\varphi - t \\ \theta - \pi - \pi\sin\lambda_1 \\ \varphi - 0 - (\pi/2)\sin\lambda_2 \\ s - 0 - \sin\lambda_3 \\ t - 0 - \sin\lambda_4 \end{bmatrix} = 0 \tag{69}$$

where $\mathbf{q} = [\theta\ \varphi\ s\ t\ \lambda_1\ \lambda_2\ \lambda_3\ \lambda_4]^T$. The Jacobian is computed as

$$\mathbf{H}_q(\mathbf{q}) = \begin{bmatrix} -\sin\theta\cos\varphi & -\cos\theta\sin\varphi & -1 & 0 & 0 & 0 & 0 & 0 \\ \cos\theta\cos\varphi & -\sin\theta\sin\varphi & 0 & 0 & 0 & 0 & 0 & 0 \\ 0 & \cos\varphi & 0 & -1 & 0 & 0 & 0 & 0 \\ 1 & 0 & 0 & 0 & -\pi\cos\lambda_1 & 0 & 0 & 0 \\ 0 & 1 & 0 & 0 & 0 & -(\pi/2)\cos\lambda_2 & 0 & 0 \\ 0 & 0 & 1 & 0 & 0 & 0 & -\cos\lambda_3 & 0 \\ 0 & 0 & 0 & 0 & 0 & 0 & 0 & -\cos\lambda_4 \end{bmatrix} \tag{70}$$

An initial guess for a point on one of the surfaces is provided as

$$\mathbf{q}^1 = [\pi\ 0\ 0.5\ 0.5\ 0\ 0\ \pi/6\ \pi/6]^T$$

Using the Moore–Penrose pseudo-inverse, and after six iterations, a starting point is found such that

$$\mathbf{q}^* = [1.571\ 0\ 0\ 0\ -0.523\ 0\ 0\ 0]^T$$

This is the exact tangent point, and is an isolated point of intersection, thus $\mathbf{q}^\circ = \mathbf{q}^*$. To verify that this is the only point of intersection, this point is substituted into the Jacobian such that $\mathbf{H}_q$ becomes row-rank deficient. Substituting $\mathbf{q}^\circ$ into the Jacobian, and performing elementary row operations yield the second row of $\mathbf{H}_q(\mathbf{q}^\circ)$ being zero. The matrix $\mathbf{F}_q(\mathbf{q}^\circ)$ is formed as

$$\mathbf{F}_q(\mathbf{q}^\circ) = \begin{bmatrix} -1 & 0 & -1 & 0 & 0 & 0 & 0 & 0 \\ 0 & 1 & 0 & -1 & 0 & 0 & 0 & 0 \\ 1 & 0 & 0 & 0 & -\pi\cos(-0.523) & 0 & 0 & 0 \\ 0 & 1 & 0 & 0 & 0 & -1.571 & 0 & 0 \\ 0 & 0 & 1 & 0 & 0 & 0 & -1 & 0 \\ 0 & 0 & 0 & 1 & 0 & 0 & 0 & -1 \end{bmatrix} \tag{71}$$

The nullspace is computed as $\boldsymbol{\tau}_1 = [-1\ 0\ 1\ 0\ -0.367\ 0\ 1\ 0]^T$ and $\boldsymbol{\tau}_2 = [0\ 1\ 0\ 1\ 0\ 0.636\ 0\ 1]^T$. Since the second row of $\mathbf{H}_q(\mathbf{q}^\circ)$ is deleted to form $\mathbf{F}_q(\mathbf{q}^\circ)$, then

$$f(\mathbf{q}) = \sin\theta\cos\varphi - 1 \tag{72}$$

The Hessian is computed and evaluated at $\mathbf{q}^\circ$. The coefficients Λ_{11}, Λ_{12}, and Λ_{22} are computed as $\Lambda_{11} = -1$, $\Lambda_{12} = 0$, and $\Lambda_{22} = -1$. The quadratic equation becomes

$$-1\alpha_1^2 - 1\alpha_2^2 = 0 \tag{73}$$

There are no real solutions to Equation 73. Therefore, there are no tangents at this point which signifies that $\mathbf{q}^\circ$ is an isolated intersection point.

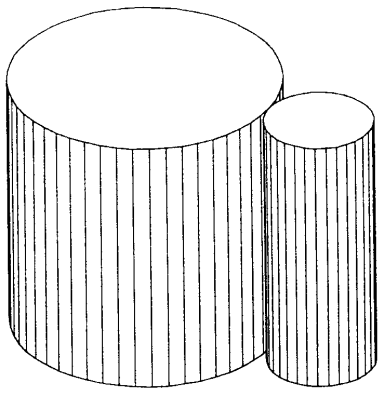

Figure 7 The intersection curve of two surfaces along their generatrix

Intersection curve is along a geometrix

This example is similar to the one discussed in Barnhill[10]. Consider the intersection of two cylinders along a generatrix as shown in *Figure 7*. It will be shown that the method presented in this paper is valid for this type of cases without any modification. Consider the first surface parametrized as

$$\mathbf{x}^1(u,v) = \begin{bmatrix} 5\cos u \\ 5\sin u \\ v \end{bmatrix}, 0 \le u \le 2\pi, \; -5 \le v \le 5 \quad (74)$$

and the surface of the second cylinder is parametrized as

$$\mathbf{x}^2(s,t) = \begin{bmatrix} 2\cos s \\ 2\sin s + 7 \\ t \end{bmatrix}, 0 \le s \le 2\pi, \; -5 \le t \le 5 \quad (75)$$

The constraint functions is written as

$$\mathbf{H}(\mathbf{q}) = \begin{bmatrix} 5\cos u - 2\cos s \\ 5\sin u - 2\sin s - 7 \\ v - t \\ u - \pi - \pi\sin\lambda_1 \\ v - 0 - 5\sin\lambda_2 \\ s - \pi - \pi\sin\lambda_3 \\ t - 0 - 5\sin\lambda_4 \end{bmatrix} = \mathbf{0} \quad (76)$$

Using the Moore–Penrose pseudo-inverse, a starting point is computed as

$$\mathbf{q}^* = [(\pi/2)\; 2.5\; (3\pi/2)\; 2.5\; (-\pi/6)\; (\pi/6)\; (\pi/6)\; (-\pi/6)]^T$$

The Jacobian is computed and evaluated at $\mathbf{q}^*$. The Jacobian is row-rank deficient (second row is zero), thus $\mathbf{q}^o = \mathbf{q}^*$. The matrix $\mathbf{F}_q(\mathbf{q})$ is formed which has rank $(n-2) = 6$. The null space of $\mathbf{F}_q(\mathbf{q})$ yields two distinct nonzero solutions

$$\tau_1 = [-0.4\; 0\; 1\; 0\; -0.147\; 0\; 0.367\; 0]^T$$

and

$$\tau_2 = [0\; 4.330\; 0\; 4.330\; 0\; 1\; 0\; 1]^T$$

Since the second row of $\mathbf{H}_q(\mathbf{q})$ was deleted to form $\mathbf{F}_q(\mathbf{q})$, then

$$f(\mathbf{q}) = 5\sin u - 2\sin s - 7 \quad (77)$$

The Hessian is evaluated at $\mathbf{q}^*$, and the coefficients Λ_{11}, Λ_{12}, and Λ_{22} are computed as $\Lambda_{11} = -14/5$, $\Lambda_{12} = 0$, and $\Lambda_{22} = 0$. The quadratic equation is determined as

$$\frac{-14}{5}\alpha_1^2 = 0 \quad (78)$$

The only solution to this equation is $\alpha_1 = 0$ and α_2 is arbitrary ($\alpha_2 = 1.0$). The only tangent vector at this point is

$$\mathbf{t}(\mathbf{H}_q) = \alpha_1\tau_1 + \alpha_2\tau_2 = [0\; 4.33\; 0\; 4.33\; 0\; 1\; 0\; 1]^T$$

Thus, the intersection curve is traced only along the line segment.

CONCLUSIONS

The formulation for tracing intersection curves between two parametric surfaces was presented. The determination of a starting point on a curve of intersection was performed using the Moore–Penrose pseudo-inverse method. Determination of bifurcation points along traced curves was performed using a row-rank deficiency criteria of the Jacobian. Calculating the bifurcation point as well switching from one branch to another was also presented. The code was demonstrated using examples where two surfaces are intersected and two tangents at the bifurcation point are computed. Special-case examples such as intersection of two surfaces at a singular point and the intersection along a generatrix were also evaluated. The efficiency of this method against other well-known methods was not addressed, neither was the computation of higher-order singularities.

ACKNOWLEDGEMENT

This research was supported by the NSF-Army Industry/University Cooperative Research Centre I/UCRC at the Center for Computer Aided Design.

REFERENCES

1 Muellenheim, G 'On determining start points for a surface/surface intersection algorithm' *Comput. Aided Geom. Des.* Vol 8 No 5 (1991) pp 401–408

2 Barnhill, R E, Farin, G, Jordan, M and Piper, B R 'Surface/surface intersection' *Comput. Aided Geom. Des.* Vol 4 (1987) pp 3–16

3 Barnhill, R E and Kersey, S N 'A marching method for parametric surface/surface intersection' *Comput. Aided Geom. Des.* Vol 7 (1989) pp 257–280

4 Farouki, R T 'The characterization of parametric surface sections' *Comput. Vis., Graph., & Image Proc.* Vol 33 (1986) pp 209–236

5 Sedeberg, T W 'Planar piecewise algebraic curves' *Comput. Aided Geom. Des.* Vol 1 (1984) pp 241–255

6 Varady, T 'Surface–surface intersections for double-quadratic parametric patches in a solid modeller' *Proc. UK–Hungarian Seminar on Computational Geometry for* CAD/CAM Cambridge University, Cambridge, UK (1983)

7 Rossignac, J R and Requicha, A A 'Piecewise circular curves for geometric modeling' *IBM J. Res. Develop.* Vol 31 (1987) pp 296–313

8 Pratt, M J and Geisow, A D 'Surface/surface intersection problems' *in* Gregory, J A (Ed.) *The Mathematics of Surfaces*, Clarendon Press, Oxford (1986) Vol 6 pp 117–142

9 Qiulin, D and Davies, B J *Surface Engineering Geometry for Computer-Aided Design and Manufacturing* Ellis Horwood UK (1987)

10 Barnhill, R E *Geometry Processing for Design and Manufacturing* SIAM (1992)

11 Hoffman, C M *Geometry and Solid Modeling, An Introduction* Morgan Kaufmann, San Mateo, CA (1989)

12 Wilf, I and Manor, Y 'Quadric-surface intersection curves: shape and structure' *Comput.-Aided Des.* Vol 25 No 10 (1993) pp 633–643

13 Markot, R P and Magedson, R L 'Procedural method for evaluating the intersection curves of two parametric surfaces' *Comput.-Aided Des.* Vol 23 No 6 (1991) pp 395–404

14 Chang, L C, Bein, W W and Angel, E 'Surface intersection using parallelism' *Comput. Aided Geom. Des.* Vol 11 No 1 (1994) pp 39–69

15 Burger, H and Schaback, R 'Parallel multistage method for surface/surface intersection' *Comput. Aided Geom. Des.* Vol 10 No 3–4 (1993) pp 277–291

16 Gleicher, M and Kass, M 'Interval refinement technique for surface intersection' *Proc. Graphics Interface* Toronto, Canada (1992) pp 242–249

17 Cheng, K P, 'Using plane vector fields to obtain all the intersection curves of two general surfaces' *in* Strasser, W and Seidel, H (Eds.) *Proc. Theory and Practice of Geometric Modeling* Springer-Verlag, New York (1988) pp 187–204

18 Aomura, S and Uehera, T 'Intersection of arbitrary surfaces' *J. Jpn Soc. Prec. Engng* Vol 57 No 9 (1991) pp 1673–1679

19 Hoffmann, C M 'A dimensionality paradigm for surface interrogations' *Comput. Aided Geom. Des.* Vol 7 (1988) pp 517–532

20 Hoffmann, C M 'Algebraic and numerical techniques for CAGD' *in* Dahmen, W, Gasca, M and Micchelli, C (Eds.) *Computations of Curves and Surfaces* NATO ASI Series C, Vol 307, Kluwer Academic (1990) pp 499–528

21 Chuang, J H and Hoffmann, C M 'On local implicit approximations of curves and surfaces' *ACM Trans. Comput. Graphics* Vol 8 (1989) pp 298–324

22 Bajaj, C L, Hoffman, C M, Lynch, R E and Hopcroft, J E H 'Tracing surface intersections' *Comput. Aided Geom. Des.* Vol 5 (1988) pp 285–307

23 Montaudouin, W T, Tiller, W and Vold, H 'Applications of power series in computational geometry' *Comput.-Aided Des.* Vol 18 (1986) pp 514–524

24 Owen, J and Rockwood, A 'Intersection of general implicit surfaces' *in* Farin, G (Ed.) *Geometric Modeling, Algorithms and Trends* SIAM Publications, Philadelphia, PA (1987)

25 Rheinboldt, W C *Numerical Analysis of Parametrized Nonlinear Equations* John Wiley, New York (1986)

26 Keller, H B *Lectures on Numerical Methods in Bifurcation Problems* Springer Verlag, Berlin (1987)

27 Allgower, E L and Georg, K *Numerical Continuation Methods* Springer-Verlag, Berlin (1990)

28 Haug, E J, Luh, C M, Adkins, F and Wang, J Y 'Numerical algorithms for mapping boundaries of manipulator workspaces' *Proc. 24th ASME Mechanisms Conf.* (1994)

29 Georg, K 'On tracing an implicitly defined curve by quasi-Newton steps and calculating bifurcation by local perturbation' *SIAM J. Sci. Statist. Comput.* No 2 (1981) pp 35–50

30 Akin, J E *Computer Assisted Mechanical Design* Prentice Hall, Englewood Cliffs, NJ (1990)

31 Noble, B and Daniel, J W *Applied Linear Algebra* Prentice-Hall, Englewood Cliffs, NJ (1988)

32 Allgower, L A and Georg, K 'Numerically stable homotopy methods without an extra dimension' Allgower and Georg (Eds.) *Lectures in Applied Mathematics Vol 26* (1990) pp 1–13

33 Cugini, A, Radi, S and Rizzi, C 'A system for parametric surface intersection' *in* Bowyer, A (Ed.) *Computer-Aided Surface Geometry and Design, The Mathematics of Surfaces IV* Oxford University Press (1994) pp 231–242

34 Golubitsky, M, Stewart, I and Schaeffer, D G *Singularities and Groups in Bifurcation Theory, Vol II* Springer Verlag, Berlin (1988)

35 Lukacs, G 'Simple singularities in surface–surface intersections' *in* Bowyer, A (Ed.) *Computer-Aided Surface Geometry and Design, The Mathematics of Surfaces* Oxford University Press (1994) pp 213–230

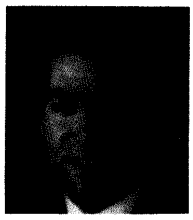

Karim Abdel-Malek is an assistant professor of mechanical engineering at the University of Iowa. He received his BS degree from the University of Jordan and his MS and PhD degrees from the University of Pennsylvania, both in mechanical engineering. Dr Abdel-Malek consulted for the manufacturing industry for a number of years before joining the faculty at the University of Iowa. His research interests include CAD/CAM *systems, robotics, dynamics and machine design.*

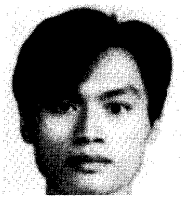

Harn-Jou Yeh is a PhD candidate in the Department of Mechanical Engineering at the University of Iowa. Mr Yeh received his BS degree from the National Taiwan University and his MS degree from the University of Iowa. He has worked for a number of years for the Center of Computer Aided Design. Mr Yeh's research interests are in kinematics, CAD *systems, and robotics.*